ORGANOMETALLICS

Article pubs.acs.org/Organometallics

Radical Capture at Nickel(II) Complexes: C-C, C-N, and C-O Bond **Formation**

Abolghasem Gus Bakhoda, Stefan Wiese, Christine Greene, Bryan C. Figula, Jeffery A. Bertke, and Timothy H. Warren*



Cite This: Organometallics 2020, 39, 1710-1718



ACCESS I

Metrics & More

Article Recommendations

s Supporting Information

ABSTRACT: The dinuclear β -diketiminato Ni^{II} tert-butoxide {[Me₃NN]Ni}₂(μ -O^tBu)₂ (2), synthesized from [Me₃NN]Ni(2,4-lutidine) (1) and di-tert-butylperoxide, is a versatile precursor for the synthesis of a series of Ni^{II} complexes [Me₃NN]Ni-FG (FG = functional group) to illustrate C-C, C-N, and C-O bond formation at Ni^{II} via radical capture. $\{[Me_3NN]Ni\}_2(\mu-O^tBu)_2$ reacts with nitromethane, alkyl and aryl amines, acetophenone, benzamide, ammonia, and phenols to deliver the corresponding mono- or dinuclear [Me3NN]Ni-FG species (FG = O2NCH2, R-NH, ArNH, PhC(O)NH, PhC(O)CH₂, NH₂, and OAr). Many of these Ni^{II} complexes are capable of capturing the benzylic radical PhCH(*)CH₃ to deliver the corresponding



PhCH(FG)CH₃ products featuring C-C, C-N, or C-O bonds. Density functional theory studies shed light on the mechanism of these transformations and suggest two competing pathways that depend on the nature of the functional groups. These radical capture reactions at [Ni^{II}]-FG complexes outline key C-C, C-N, and C-O bond forming steps, foreshadowing families of nickel radical relay catalysts.

■ INTRODUCTION

Nickel complexes serve as highly effective catalysts for crosscoupling reactions. Alongside palladium, nickel has been used extensively for both Suzuki-Miyaura and Negishi crosscouplings.² Over the past few decades, the scope of crosscoupling reactions has improved well beyond more conventional biaryl synthesis and now includes several types of coupling partners. For instance, Ni-catalyzed protocols for C_{sp}³-C_{sp}³ bond formation with alkyl halides and organic nucleophiles bound to Mg, B, Si, Zn, Sn, and Zr can furnish high yields along with high stereoselectivity in some cases (Figure 1a).³

Nickel catalysis also enables cross-electrophile coupling between sp³ and sp² as well as sp³ electrophiles (Figure 1b). ^{4a–i} A commonly accepted mechanism involves the oxidative addition of R-X that generates a X-[Ni^{II}]-R species followed by attack of an alkyl radical R' generated from R'-X' under reductive conditions to give the R-R' coupled product. These reactions can also proceed via metallaphotoredox conditions that generate the alkyl radical R' from carboxylic acids, organoborate salts, alkylsilicates, and aryl halides, as well as from sp³ C-H bonds via H atom abstraction (Figure 1c). 4g-r Attack of the alkyl radical R' on X-[Ni^{II}]-R provides a Ni^{III} complex $X-[Ni^{III}](R)(R')$ susceptible to reductive elimination (Figure 1d). Alternatively, this Ni^{III} intermediate can be generated from a Ni^I organometallic [Ni^I]-R' upon the oxidative addition of R-X.4s-u In either case, the coupling partners assemble to form a Ni^{III} intermediate that enables R-R' bond formation.

As C_{sp}³-H bonds are ubiquitous in organic molecules, discovering new methods to carry out C_{sp}³-H functionalization opens new opportunities to modify existing molecules. Several C_{sp}³-H functionalization protocols catalyzed by firstrow transition metals such as Mn, 5 Fe, 6 Co, 7 Ni, 8 and Cu 9 are proposed to proceed via capture of an organic C-based radical (R*) by the metal center [M]-FG (where FG is the desired functional group) to furnish the organic product R-FG. In particular, several groups have successfully used nickel as an efficient catalyst for C_{sp}^3 -H functionalization to form C_{sp}^3 -C and C_{sp}³-N bonds via a radical-relay mechanism (Figure 2).⁸ For instance, Ni(acac)₂ has been used as an effective catalyst in $C_{sp}{}^{3}-C_{sp}{}^{2}$ bond formation in the presence of ${}^{t}BuOO{}^{t}Bu$ as an external oxidant (Figure 2a,b).8 Similarly, Ni(acac)₂ was shown to be an effective catalyst for N-alkoxyamidation of simple aliphatic hydrocarbons under oxidative conditions (Figure 2f).8f Recently, alkynylation of simple (cyclo)alkanes with terminal alkynes has been reported via a multimetal catalyzed reaction strategy in which $C_{sp}^{3}-C_{sp}$ bond formation takes place at Ni (Figure 2e). 8a,c While these C-H functionalization reactions are not as mechanistically well-defined, alkyl radicals R[•] are thought to be involved en route to R-FG formation.

Received: January 11, 2020 Published: April 30, 2020





Figure 1. Ni-catalyzed cross-coupling reactions.

Figure 2. C_{sp} :—H functionalization catalyzed by Ni through alkyl radical capture.

The longest known system for catalytic C-H functionalization that involves radical capture is the copper-catalyzed

Khasrasch-Sosnovky reaction. Seminal work by Kharasch and Sosnovsky introduced Cu as an effective catalyst for the formation of C-O bonds from a peroxyester. ⁹ In the presence of cuprous salts, tert-butyl perbenzoate (*BuO-OC(O)Ph) reacts with various olefins to construct new C_{sp}^3 -O bonds in the corresponding allylic benzoates.⁹ It is thought that a radical R[•] generated via H atom abstraction of R-H from an alkoxy radical reacts with a [Cu^{II}]-FG complex to deliver R-FG products. Kochi demonstrated that a range of Cu^{II} complexes containing the anions FG⁻ (FG = O₂CR, Cl, Br, I, SCN, N₃, and CN) lead to R-FG bond formation. ¹⁰ More recently, we have unequivocally demonstrated radical capture by [Cu^{II}]-FG complexes (FG = anilide, phenoxide) formed by acid-base reaction between [Cu^{II}]-O^tBu and H-NHAr or Ac-OAr enables C-H amination and etherification (Figure 3).11 Such radical-relay mechanisms have also been used for C-C bond formation.

$$[Cu^{|I}]\text{-NH-2-py} + \bullet CPh_3 \longrightarrow Ph_3C \longrightarrow NH-2-py$$

$$78\%$$

$$Gomberg's \ dimer \quad 2-py = 2-pyridyI$$

$$[Cu^{|I}]\text{-OAr}^{4Cl} + \bullet CMe_3 \longrightarrow Me_3C \longrightarrow OAr^{4Cl}$$

$$71\%$$

$$^{\prime}BuN=N^{\prime}Bu \qquad Ar^{4Cl} = 4-ClC_6H_4$$

$$R = Cl \ in \ C-H \ amination$$

$$R = OMe \ in \ C-H \ etherification$$

$$This \ work:$$

$$[Ni^{|I}]\text{-FG} + Ph \longrightarrow Ph$$

$$A \cap N_2 \cap N_1$$

$$[Ni^{|I}]\text{-FG} + Ph \longrightarrow Ph$$

$$[Me_3NN]Ni$$

Figure 3. Top: C-N and C-O bond formation by radical capture at a copper(II) anilide and phenolate. Bottom: Radical capture at related Ni^{II} complexes investigated in this work.

To expand the scope of functional groups that can be installed via sp³ radicals, we were intrigued by the possibility of related radical capture reactions at corresponding nickel complexes [Ni^{II}]-FG (Figure 3). We hypothesized that such nickel complexes could generally be more thermally stable than corresponding [Cu^{II}]-FG complexes that can be prone to reduction to [Cu^I], either via H atom abstraction to form H-FG^{11c} or via formation of FG-FG bonds (e.g., FG = NHPh). 11g This study outlines a general pathway for the formation of a wide range of [NiII]-FG species from a common $[Ni^{II}]_2(\mu-O^tBu)_2$ intermediate that features a basic tert-butoxide group that enables facile acid-base reactions with a range of H-FG species. Many of these [Ni^{II}]-FG species undergo radical capture with the PhCH(*)Me radical, foreshadowing new potential families of nickel catalysts for radical relay reactions.

■ RESULTS AND DISCUSSION¹³

Synthesis and Characterization of Dinuclear Nickel(II) *tert*-Butoxide 2. Since β -diketiminato $[Cu^{II}]$ - O^tBu complexes allow for acid-base reactions with diverse H-FG species to form $[Cu^{II}]$ -FG intermediates that function in

radical relay catalysis,¹¹ we sought the synthesis of the corresponding nickel analogue. Addition of excess ${}^{t}BuOO{}^{t}Bu$ to a solution of nickel(I) complex [Me₃NN]Ni(2,4-lutidine) (1)¹⁴ in Et₂O at RT results in the precipitation of the Ni^{II} alkoxide {[Me₃NN]Ni}₂(μ -O ^{t}Bu), (2) in 82% isolated yield as

$$2 \underbrace{\begin{array}{c} N_{i}(lut) \\ N_{i}(lut) \\ N_{i}(lut) \\ N_{i}(lut) \\ R_{i}(lut) \\ R_{i}(l$$

Figure 4. Synthesis and crystal structure of complex 2.

a dark green solid (Figure 4). Slow vapor diffusion of ^tBuOO^tBu into a toluene solution of 1 forms dark green crystals suitable for single-crystal X-ray diffraction. The solidstate structure of dinuclear 2 consists of two monomeric [Me₂NN]Ni^{II}-O^tBu units in which the two Ni centers are related by an inversion center with a Ni···Ni separation of 3.058 Å (Figure 4). Complex 2 exhibits pseudotetrahedral coordination at Ni with twist angles between N-Ni-N and O-Ni-O planes of 83.01° and Ni-O distances of 1.9527(14) and 1.9828(14) Å. Dinuclear 2 is structurally similar to $\{[Me_3NN]Ni\}_2(\mu\text{-OCy})_2$ (Cy = cyclohexyl) originally synthesized by reaction of ONOCy with [Me₃NN]Ni^I(lut). 15 As suggested by its tetrahedral geometry around the Ni center, complex **2** is paramagnetic in solution with a μ_{eff} of 3.3(4) B.M. in toluene- d_8 by the Evans method, ¹⁶ indicating some degree of antiferromagnetic coupling.

Despite the dinuclear nature that renders it rather insoluble in common hydrocarbon solvents, **2** reacts readily with a number of mildly acidic substrates H–FG to provide mononuclear [Ni^{II}]–FG and dinuclear [Ni^{II}]₂(μ -FG)₂ com-

plexes (FG = NO_2CH_2 , $CH_2C(O)Ph$, NHC(O)Ph, NHAr, NHR, or OAr) as illustrated in Figure 5.

Synthesis and Characterization of Mononuclear Nickel(II) Nitromethanoate 3, Enolate 4, and Benza**mide 5.** { $[Me_3NN]Ni$ }₂(μ -O^tBu)₂ (2) reacts with nitromethane to form mononuclear complex $[Me_3NN]Ni(\kappa^2$ O₂N=CH₂) (3) isolated as red crystals from ether in 78% (Figure 6a). Complex 3 exhibits a somewhat unusual O₁O'nitromethanoato coordination mode¹⁷ that gives rise to square planar coordination at the Ni^{II} center. The Ni-O distances in 3 are 1.9064(13) and 1.9281(13) Å with O-N-O and O-Ni-O angles of 110.03(14)° and 69.20(5)°, respectively (Figure 6a). The C=N distance is significantly shortened to 1.280(2) Å that indicates substantial C=N double-bond character as compared to a normal C-N single bond at 1.47 Å (Figure 6a). This square planar complex is diamagnetic whose NMR spectra in benzene- d_6 exhibit effective $C_{2\nu}$ symmetry. The IR spectrum of 3 shows $\nu_{
m NO}$ bands at 1608 and 1624 cm $^{-1}$ along with $\nu_{\rm C=N}$ at 1529 cm⁻¹ in accordance with reported literature values.

Upon reaction with 2 equiv of acetophenone, complex 2 furnishes $[Me_3NN]Ni(\eta^3-CH_2C(O)Ph)$ (4) as yellow crystals from ether in 60% isolated yield. While there are several early transition-metal—enolate structures with either κ^2 - or η^3 -Obinding coordination bonding modes, 18 complex 4 is a particularly rare, first-row transition-metal-enolate with both O- and C-coordination, joined by only [NNN]Cu(κ^1 -OC(C= C(Me)Ph) recently reported by Tolman. 18c The phenyl enolate ligand binds to the nickel center through an η^3 interaction involving the O,C, and C atoms in the delocalized π -system. The Ni-C_{CH}, and Ni-O bond distances in 4 are 2.0570(16) and 1.9055(11) Å, respectively, while the Ni-C_{carbonvl} bond length is 2.0400(16) Å (Figure 6b). The IR spectrum of 4 shows a $\nu_{C=0}$ band at 1651 cm⁻¹. Similarly, 2 reacts with 2 equiv of benzamide to yield an analogous $[Me_3NN]Ni(\kappa^2-NHC(O)Ph)$ (5) complex isolated in 55% yield as brown crystals. Benzamide complex 5 exhibits square planar structure (Figure 6c) closely related to that of 4. The Ni-N_{amide} and Ni-O bond distances in 5 are 1.948(19) and 1.906(13) Å, respectively, while the Ni– $C_{carbonyl}$ bond length is 2.316(5) Å. Thus, **5** is best considered κ^2 -N,O with the Ni center only 33.95° out of the benzamide O-C-N plane,

Figure 5. Synthetic pathways for the synthesis of Ni^{II} complexes 3-11.

Figure 6. Crystal structures of complexes **3**, **4**, and **5**. Ellipsoids are shown at 50% (3 and 4) and 30% (5) probability. H atoms have been omitted for clarity with the exception of the C–H bonds in nitromethanoato and enolato ligands in **3** and **4**, respectively, as well as the amido N–H bond in **5**.

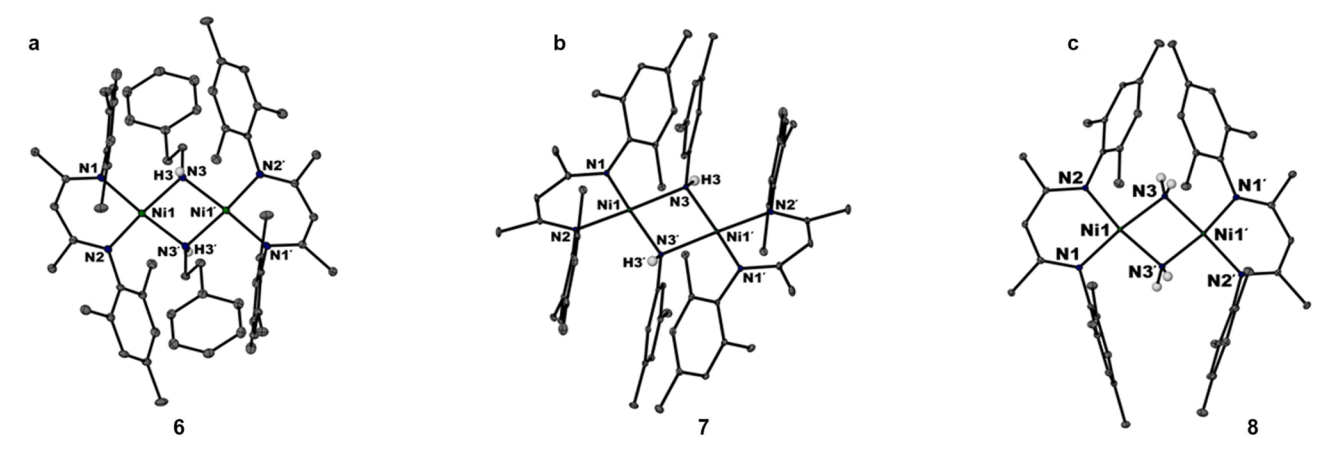


Figure 7. Crystal structures of complexes 6, 7, and 8. Ellipsoids are shown at 30% (6 and 7) and 50% (8) probability levels and hydrogen atoms have been omitted for clarity with the exception of the N–H bonds in amido and anilido ligands.

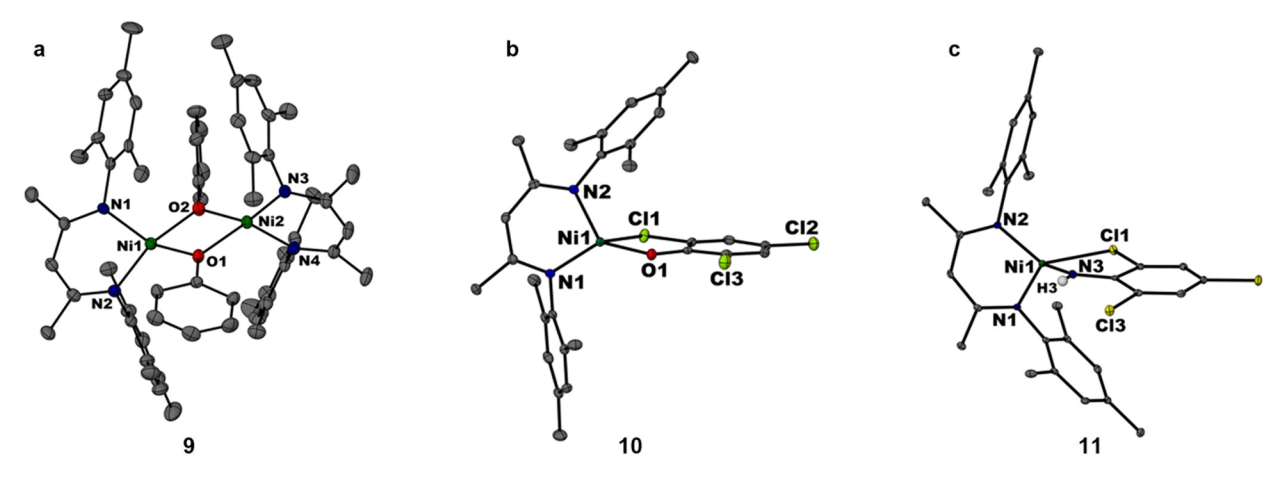


Figure 8. Crystal structures of complexes 9 (left), 10 (middle), and 11 (right). Ellipsoids are shown at 30% (9) and 50% (10 and 11) probability levels and hydrogen atoms have been omitted for clarity except the N-H bonds in the anilido ligand of 11.

whereas in η^3 -O,C,C-acetophenone enolate 4, the Ni center is 64.20° out of the enolate O-C-C plane.

Diamagnetic 4 and 5 exhibit fluxional 1 H NMR spectra in toluene- d_8 . At -80 $^{\circ}$ C, 4 and 5 each shows two sets of two distinct β -diketiminato N-aryl ortho-Me, para-Me, and backbone Me resonances (Figures S21–S22) consistent with their solid-state structure that possess two different donors in square planar 4 and 5. Warming results in coalescence of these sets of resonances indicating a symmetrization within the coordination wedge that may proceed via three-coordinate κ^1 -enolate and κ^1 -benzamide intermediates or tetrahedral κ^2 -intermediates. The barrier is higher for enolate derivative 4 than for

benzamide **5** with $\Delta G^{\ddagger}(288 \text{ K}) = 13.9(4) \text{ kcal/mol}$ and $\Delta G^{\ddagger}(207 \text{ K}) = 10.3(2) \text{ kcal/mol}$, respectively (Figures S21 and S22).

Synthesis and Characterization of Dinuclear Nickel(II) Alkylamide 6, Anilide 7, and Parent Amide 8. Both phenethylamine and 3,5-dimethylamiline undergo an acid—base reaction with 2 to provide dinuclear complexes {[Me₃NN]-Ni}₂(μ -NHCH₂CH₂Ph)₂ (6) and {[Me₃NN]Ni}₂(μ -NHPh^{3,5-Me2})₂ (7) isolated as red crystals in 58 and 62% yields, respectively (Figures 7a,b). X-ray structures of 6 and 7 reveal dinuclear, slightly distorted square planar structures bridged by amide or anilide ligands to give Ni centers related

by inversion symmetry with Ni···Ni separations of 2.949 and 2.998 Å, respectively (Figures 7a,b). The Ni-Namido distances in 6 are 1.918(3) and 1.922(3) Å, whereas 7 shows Ni-Namido bond lengths of 1.9462(13) and 1.9551(13) Å. In both complexes 6 and 7, the Ni centers adopt a twisted square planar geometry with angles of 20.02 and 22.14° between the N $_{\beta\text{-dik}}$ -Ni-N $_{\beta\text{-dik}}$ and opposing N3-Ni-N3′ planes, respectively. In solution, 7 is diamagnetic and possesses a ^1H NMR spectrum in C $_6\text{D}_6$ at room temperature (Figure S15) that features a β -diketiminato C-H backbone resonance at δ 4.51 ppm with two different signals for the β -diketiminato N-aryl meta-Ar-H sites at δ 6.880 and 6.464 ppm. Thus, 7 maintains its dimeric, square-planar structure in solution at room temperature with one anilido NAr $^{\text{Me2}}$ group above and below the N3-Ni-N3′ plane.

A particularly novel complex, the parent amido species $\{[Me_3NN]Ni\}_2(\mu-NH_2)_2$ (8), was isolated in 91% yield as orange crystals by slow diffusion of NH_3 into a solution of $\{[Me_3NN]Ni\}_2(\mu-O^tBu)_2$ (2) (Figure 8c). As compared to dinuclear amido complexes 6 and 7, parent amide 8 possesses the shortest $Ni-N_{amide}$ bond distances of 1.9001(11) and 1.9017(11) Å that result in a shortened $Ni\cdots Ni$ separation of 2.919 Å (Figure 7c). The twist angle between the $N_{\beta-dik}-Ni-N_{\beta-dik}$ and $N_{amide}-Ni-N_{amide}$ planes of 18.42° deviates least from idealized square planar geometry, likely a result of the minimal steric demands of the amido ligands. Unfortunately, 8 is not soluble in organic solvents even at elevated temperatures, which hampers its solution characterization. FT-IR spectrum of 8 shows two peaks at 3430 and 3413 cm⁻¹ as a result of two N-H stretching modes of the amido ligand.

Synthesis and Characterization of Dinuclear and Mononuclear Nickel(II) Phenolates 9 and 10 and Mononuclear Anilide 11. Nickel(II) complexes $[Ni^{II}]$ –FG that bear weaker donors give rise to dinuclear or mononuclear species that are paramagnetic. For instance, addition of 2 equiv of phenol to $\{[Me_3NN]Ni\}_2(\mu\text{-}OBu^t)_2$ (2) in ether at RT gives the dinuclear phenoxide complex $\{[Me_3NN]Ni\}_2(\mu\text{-}OPh)_2$ (9) as dark green crystals (Figure 8a). The X-ray structure of 9 reveals a distorted tetrahedral environment around the Ni^{II} centers with Ni–O distances of 1.966(3) and 1.967(3) Å along with a Ni···Ni separation of 3.115 Å, which is the longest in the series of dinuclear complexes 6, 7, and 8 (Figures 8a–c). This complex is paramagnetic in solution with a $\mu_{\rm eff}$ of 2.7(2) B.M. in benzene- d_6 by the Evans method. ¹⁶

Addition of the bulky, electron-poor 2,4,6-trichlorophenol or 2,4,6-trichloroaniline to 2 provided deep blue $[Me_3NN]Ni-OPh^{2,4,6-Cl_3}$ (10) or teal $[Me_3NN]Ni-NHPh^{2,4,6-Cl_3}$ (11) isolated in 49 and 40% yields, respectively (Figures 8b,c). These structures feature much shorter Ni-N and Ni-O distances to the anilido or phenoxy donors, 1.8765(19) and 1.8812(12) Å, respectively, than observed in the dinuclear structures of 7 and 9. Interestingly, these structures are best described as pseudotetrahedral due to coordination of one of the *ortho-Cl* atoms with Ni-Cl distances of 2.4811(6) and 2.4595(5) Å in anilido 10 and phenoxy 11, respectively. Accordingly, each is paramagnetic in solution with magnetic susceptibilities (benzene- d_6) of 2.8(1) and 2.6(2) B.M., ¹⁶ respectively. This is consistent with S=1, high-spin d⁸ electronic structures.

Capture of the PhCH(*)Me Radical by [Ni^{II}]-FG Complexes. We explored the radical capture ability of each [Me₃NN]Ni-FG complex 3-11 through the in situ generation of the secondary benzylic radical PhCH(*)Me

Ph N=N

N=N

Nes

Noill—FG + Ph

$$A_{-N_2}$$

Ph

No occ Ph

FG

No occ Ph

Ph

No occ Ph

No

Figure 9. PhCH(*)Me radical capture by [Ni^{II}]-FG complexes.

from the aliphatic azo compound (E/Z)-azobis $(\alpha$ -phenylethane) at 100 °C (Figure 9). Reaction of complexes 3–7 and 9 with (E/Z)-azobis $(\alpha$ -phenylethane) at 100 °C in fluorobenzene solvent gave 25–67% yields of the corresponding radical capture products PhCH(FG)Me. Thus, radical capture at $[Ni^{II}]$ -FG complexes results in the formation of C–C (59% for 3 and 61% for 4), C–N (67% for 5, 55% for 6, and 25% for 7), and C–O (48% for 9) bonds. In the case of complex 7, concomitant formation of diazene ArN=NAr (Ar = 3,5-Me₂C₆H₃) was observed in 49% GC yield along with 25% yield of the amination product PhCH(NHAr)Me. For the parent amide complex $\{[Me_3NN]Ni\}_2(\mu$ -NH₂) (8) only a trace amount of the C–H amination product PhCH(NH₂)Me was detected by GC-MS analysis, attributed to its poor solubility, even at elevated temperatures.

In contrast, mononuclear complexes $[Me_3NN]Ni-FG$ with bulky, electron-poor functional groups $(FG=OAr^{Cl3}\ (10)$ or $NHAr^{Cl3}\ (11))$ did not result in radical capture. Rather, only erythro and threo isomers of the ethylbenzene radical dimer PhCH(Me)-CH(Me)Ph are observed. In fact, this product of $PhCH(^{\bullet})Me$ radical dimerization occurs in comparable amounts across all reactions. Control experiments show no radical capture at room temperature after overnight stirring of the complexes with (E/Z)-azobis $(\alpha$ -phenylethane) in PhF.

Computational Analysis of Radical Capture Pathways at Nickel(II) Nitromethanoate 3 and Benzamide 5. Most mechanistic proposals for Ni-catalyzed C_{sp2} - C_{sp3} bond formation involve radical capture at Ni^{II} to form a Ni^{III} organometallic complex, followed by reductive elimination (Figures 1d and 10, route a). A less prominent mechanism involves concerted bond formation between the PhCH(*)Me radical at the functional group (Figure 10, route b). When radical capture at the functional group involves bond formation with an atom that is bound to the metal center, both radical capture at the metal center and functional group could be competitive. To illustrate this competition between radical capture pathways, we computationally considered capture of

R.
$$\begin{bmatrix} [Ni^{||}] - FG \\ R \end{bmatrix}$$

$$\begin{bmatrix} [Ni^{||}] - FG$$

Figure 10. Possible mechanistic routes for $[Ni^{II}]$ -FG radical capture in benzene.

the PhCH($^{\bullet}$)Me radical at Ni^{II} nitromethanoate 3 and benzamide 5.

DFT studies at the BP86+GD3BJ/6-311++G(d,p)/SMD-benzene// BP86/6-31+G(d)/SMD-gas level of theory consider both distinct pathways to form PhCH(FG)Me products from 3 and 5 with PhCH($^{\bullet}$)Me. In all cases, we consider the Ni^I solvento species [Me₃NN]Ni(η^2 -benzene) as the final product to assess the overall thermodynamics of radical capture. Accordingly, capture of the ethylbenzene radical by nitroalkanoate [Me₃NN]Ni^{II}(κ^2 -O₂N = CH₂) (3) and benzamide [Me₃NN]Ni(κ^2 -NHC(O)Ph) (5) is thermodynamically favored with ΔG_{rxn} = -18.2 and -8.1 kcal/mol, respectively (Figure 11).

We considered in detail the interaction of the ethylbenzene radical with nitroalkanoate 3 (Figure 11a). Radical capture at the metal center to form the Ni^{III} organometallic species [Me₃NN]Ni^{III}(κ^2 -O₂NCH₂)(CH(Ph)CH₃) is endergonic (ΔG = +5.8 kcal/mol) and possesses a barrier of 11.3 kcal/mol. However, direct capture of the radical at the C atom of the nitroalkanoate ligand in [Me₃NN]Ni^{II}(κ^2 -O₂N=CH₂) (3) is significantly exergonic to form [Me₃NN]Ni(κ^2 -O₂NCH₂-CH(CH₃)Ph) with ΔG = -15.9 kcal/mol. Importantly, this direct capture exhibits only a modest barrier of 7.5 kcal/mol, which is lower in energy than the barrier for the formation of the Ni^{III} intermediate. Thus, direct C–C bond formation at the nitromethanoate ligand is favored over initial radical capture at the metal center.

Examining the interaction of ethylbenzene radical (R^{\bullet}) with benzamide 5 (Figure 11b), we find that capture at the metal

center to form the Ni^{III} organometallic species [Me₃NN]- $Ni^{III}(\kappa^2-NHC(O)Ph)(CH(Ph)CH_3)$ is slightly endergonic at 3.2 kcal/mol with a barrier of 8.8 kcal/mol. The overall barrier for C-N bond formation comes from the reductive elimination of $[Me_2NN]Ni^{III}(\kappa^2-NHC(O)Ph)(CH(Ph)CH_2)$ at 13.6 kcal/mol. We also considered the alternative pathway with the formation of a $[Me_3NN]Ni^{III}(\kappa^1-NH(CH(Ph)CH_3)-$ C(O)Ph) intermediate via radical capture at the functional group. We took into consideration the binding of the radical at $[Me_3NN]Ni^{III}(\kappa^2-NHC(O)Ph)$ 5, but a relaxed potential energy scan found that isomerization occurred prior to radical binding. We propose that the [Me₃NN]Ni(κ^2 -NHC(O)Ph) will isomerize to form a $[Me_3NN]Ni(\kappa^1NHC(O)Ph)$ complex endergonically at +6.7 kcal/mol with a barrier of 9.4 kcal/mol (at 298 K). While other isomers of $[Me_3NN]Ni(\kappa^2-NHC(O)-$ Ph) were considered, we found that the [Me₃NN]Ni(κ^{1} -NHC(O)Ph) isomer was the most likely pathway (Scheme S3). The calculated barrier for κ^2 to κ^1 isomerization is close to the experimental value $\Delta G^{\dagger}(207 \text{ K}) = 10.3(2) \text{ kcal/mol for}$ symmetrization determined by variable temperature NMR (Figure S22). $[Me_3NN]Ni(\kappa^1-NHC(O)Ph)$ can then undergo direct radical capture at the functional group to form $[Me_3NN]Ni(NH(CH(CH_3)C(O)Ph) complex (\Delta G_{overall} =$ -6.4 kcal/mol) with an overall barrier of +14.9 which is higher in energy than the barrier for the radical capture at the metal center by 1.3 kcal/mol. While the barrier for radical capture is slightly higher in energy at the metal center than at the functional group, the difference between both pathways is within the range of error suggesting that these pathways could be competitive.

For $[Me_3NN]Ni^{II}(\kappa^2-O_2N=CH_2)$ (3) radical capture at the functional group is situated away from the metal center and thus is the thermodynamically favored pathway. For radical capture involving $[Me_3NN]Ni(\kappa^2-NHC(O)Ph)$ (5), however, a rearrangement is necessary for direct bond formation to occur at the functional group. This barrier is within the same thermodynamical range as radical capture at the metal center. The results of this DFT study indicate that the mechanism is highly dependent upon the functional group. This outlined mechanism gives new insight into the importance of the functional group in radical capture allowing for new variables to be explored to improve catalytic function.

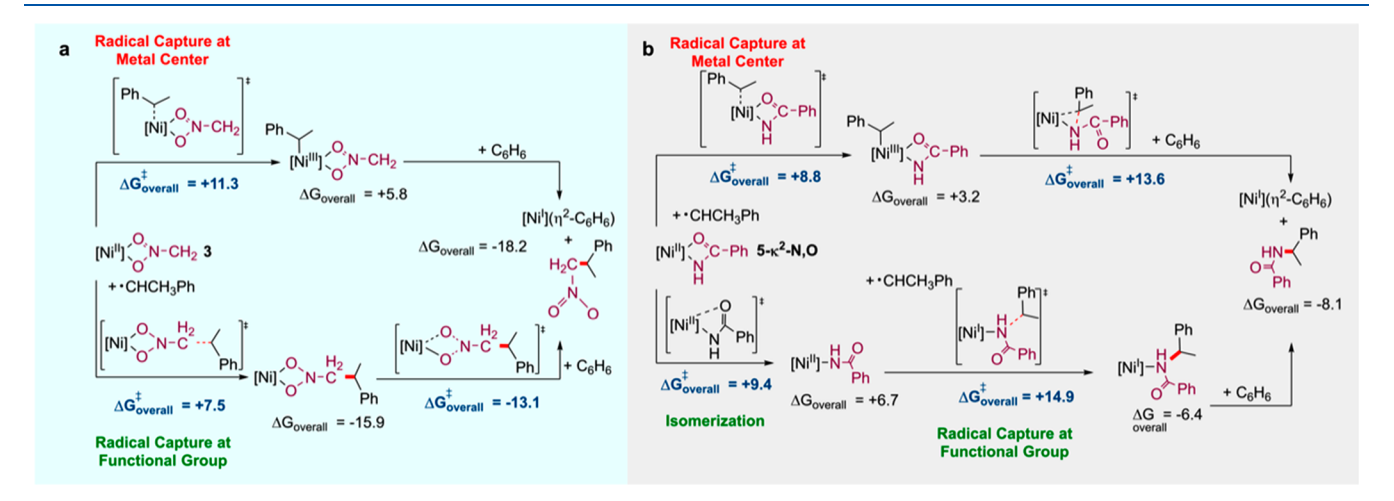


Figure 11. Possible mechanistic routes for radical capture at $[Me_3NN]Ni^{II}$ -FG complexes 3 and 5 in benzene at 298 K. Transition states that are barriers for the pathway are bolded. All metal complexes are S = 1/2 species except 3,5- κ^2 -N,O, and 5- κ^1 -N. All values are in kcal/mol at 298 K.

CONCLUSIONS

 $\{[Me_3NN]Ni\}_2(\mu-O^tBu)_2$ (2) serves as a versatile precursor for the installation of a variety of functional groups onto the β diketiminato Ni^{II} center. H-FG reagents such as ammonia, alkyl amines, anilines, nitromethane, acetophenone, benzamide, and phenols cleanly react with 2 to give mono- and dinuclear $\hat{\beta}$ -diketiminato [Ni^{II}]-FG species that may be isolated and fully characterized. Despite the considerably higher pK_a of many of the N-H and C-H bonds in substrates used to install functional groups at Ni^{II} via {[Me₃NN]Ni}₂(µ- $O^{t}Bu)_{2}$ (2) as compared to the leaving H-O^tBu, the preference of later first row metals for somewhat softer donors overcomes this unfavorable pK_a difference, in some cases assisted by chelation. Importantly, the mononuclear S = 0[Ni^{II}]-FG complexes as well as the soluble dinuclear $[Ni^{II}]_2(\mu\text{-FG})_2$ complexes capture the alkyl radical PhCH($^{\bullet}$)-CH₃ to form PhCH(FG)CH₃, clearly illustrating the ability of a range of Ni^{II} complexes [Ni^{II}]-FG to mediate C-C, C-N, and C-O bond forming steps via C_{sp}^3 radicals R^{\bullet} . Since nearly all complexes of 3-7 and 9 that undergo radical capture are reasonably stable at high temperatures required for PhCH(*)-CH₃ generation from the corresponding diazene RN=NR (Figures S23-S27), it is unlikely that alkyl radical capture proceeds via ejection of a (*)FG radical from [Ni^{II}]-FG complexes. Rather, alkyl radical capture occurs at somewhat sterically shielded [Ni^{II}]-FG complexes, further supported by the lack of radical capture when $[Ni^{II}](\kappa^2\text{-NHC}(O)Ph)$ (5) is heated with with 'BuN=N'Bu that readily generates the more hindered ^tBu(*) radical.²²

Curiously, mononuclear $S = 1 \text{ Ni}^{\text{II}}$ phenolate **10** and anilide 11 did not provide radical capture products. This suggests that their rates of radical capture are much slower than those of the other complexes bearing more electron-rich functional groups. Thus, there may be an electronic basis for the differential radical capture behavior since these mononuclear complexes do not have any obvious steric constraints against radical capture. Moreover, computational studies identify competing pathways for R-FG bond formation, indicating that radical capture at Ni^{II} to give a Ni^{III} intermediate is not always the favored pathway as commonly assumed (Figure 1). Since [Ni^{II}]-O^tBu intermediates can be formed via interaction of ^tBuOO^tBu and [Ni^I] as well as undergo facile acid-base reactions with H-FG to form key [Ni^{II}]-FG intermediates, these [Ni^{II}]-FG species provide fresh insight into an array of bond forming reactions that can be realized through C-H functionalization utilizing new nickel radial relay catalysts.

ASSOCIATED CONTENT

Supporting Information

The Supporting Information is available free of charge at https://pubs.acs.org/doi/10.1021/acs.organomet.0c00021.

Synthesis and characterization of all the compounds in this work and X-ray diffraction structures (PDF) DFT calculated Cartesian coordinates for the optimized structures (XYZ)

Accession Codes

CCDC 1861876–1861885 contain the supplementary crystallographic data for this paper. These data can be obtained free of charge via www.ccdc.cam.ac.uk/data_request/cif, or by emailing data_request@ccdc.cam.ac.uk, or by contacting The Cambridge Crystallographic Data Centre, 12 Union Road, Cambridge CB2 1EZ, UK; fax: +44 1223 336033.

AUTHOR INFORMATION

Corresponding Author

Timothy H. Warren — Georgetown University, Department of Chemistry, Washington, District of Columbia 20057-1227, United States; Occid.org/0000-0001-9217-8890; Email: thw@georgetown.edu

Authors

Abolghasem Gus Bakhoda — Georgetown University,
Department of Chemistry, Washington, District of Columbia
20057-1227, United States; orcid.org/0000-0002-3222-8873

Stefan Wiese — Georgetown University, Department of Chemistry, Washington, District of Columbia 20057-1227, United States

Christine Greene – Georgetown University, Department of Chemistry, Washington, District of Columbia 20057-1227, United States

Bryan C. Figula – Georgetown University, Department of Chemistry, Washington, District of Columbia 20057-1227, United States

Jeffery A. Bertke — Georgetown University, Department of Chemistry, Washington, District of Columbia 20057-1227, United States; Ocid.org/0000-0002-3419-5163

Complete contact information is available at: https://pubs.acs.org/10.1021/acs.organomet.0c00021

Notes

The authors declare no competing financial interest.

ACKNOWLEDGMENTS

T.H.W. is grateful to the National Science Foundation (CHE-1665348) and the Georgetown Environment Initiative for support of this work.

REFERENCES

- (1) (a) Hazari, N.; Melvin, P. R.; Beromi, M. M. Well-defined nickel and palladium precatalysts for cross-coupling. *Nat. Rev. Chem.* 2017, 1, No. 0025. (b) Tasker, S. Z.; Standley, E. A.; Jamison, T. F. Recent advances in homogeneous nickel catalysis. *Nature* 2014, 509, 299–309. (c) Yamaguchi, J.; Muto, K.; Itami, K. Recent Progress in Nickel-Catalyzed Biaryl Coupling. *Eur. J. Org. Chem.* 2013, 2013, 19–30. (d) Rosen, B. M.; Quasdorf, K. W.; Wilson, D. A.; Zhang, N.; Resmerita, A.-M.; Garg, N. K.; Percec, V. Nickel-Catalyzed Cross-Couplings Involving Carbon—Oxygen Bonds. *Chem. Rev.* 2011, 111, 1346–1416. (e) Hassan, J.; Sévignon, M.; Gozzi, C.; Schulz, E.; Lemaire, M. Aryl—Aryl Bond Formation One Century after the Discovery of the Ullmann Reaction. *Chem. Rev.* 2002, 102, 1359–1469.
- (2) Han, F.-S. Transition-metal-catalyzed Suzuki-Miyaura cross-coupling reactions: a remarkable advance from palladium to nickel catalysts. *Chem. Soc. Rev.* **2013**, *42*, 5270–5298.
- (3) (a) Fu, G. C. Transition-Metal Catalysis of Nucleophilic Substitution Reactions: A Radical Alternative to S_N1 and S_N2 Processes. ACS Cent. Sci. 2017, 3, 692–700. (b) Choi, J.; Fu, G. C. Transition metal—catalyzed alkyl-alkyl bond formation: Another dimension in cross-coupling chemistry. Science 2017, 356, No. eaaf7230. (c) Lou, S.; Fu, G. C. Enantioselective Alkenylation via Nickel-Catalyzed Cross-Coupling with Organozirconium Reagents. J. Am. Chem. Soc. 2010, 132, 5010–5011.
- (4) (a) Weix, D. J. Methods and Mechanisms for Cross-Electrophile Coupling of Csp² Halides with Alkyl Electrophiles. *Acc. Chem. Res.* **2015**, *48*, 1767–1775. (b) Ackerman, L. K. G.; Anka-Lufford, L. L.; Naodovic, M.; Weix, D. J. Cobalt co-catalysis for cross-electrophile coupling: diarylmethanes from benzyl mesylates and aryl halides.

Chem. Sci. 2015, 6, 1115-1119. (c) Everson, D. A.; Weix, D. J. Cross-Electrophile Coupling: Principles of Reactivity and Selectivity. J. Org. Chem. 2014, 79, 4793-4798. (d) Biswas, S.; Weix, D. J. Mechanism and Selectivity in Nickel-Catalyzed Cross-Electrophile Coupling of Aryl Halides with Alkyl Halides. J. Am. Chem. Soc. 2013, 135, 16192-16197. (e) Everson, D. A.; Jones, B. A.; Weix, D. J. Replacing Conventional Carbon Nucleophiles with Electrophiles: Nickel-Catalyzed Reductive Alkylation of Aryl Bromides and Chlorides. J. Am. Chem. Soc. 2012, 134, 6146-6159. (f) Everson, D. A.; Shrestha, R.; Weix, D. J. Nickel-Catalyzed Reductive Cross-Coupling of Aryl Halides with Alkyl Halides. J. Am. Chem. Soc. 2010, 132, 920-921. (g) Twilton, J.; Le, C.; Zhang, p.; Shaw, M. H.; Evans, R. W.; MacMillan, D. W. C. Earth-Abundant Transition Metal Catalysts for Alkene Hydrosilylation and Hydroboration: Opportunities and Assessments. Nat. Rev. Chem. 2017, 1, No. 0052. (h) Nielsen, M. K.; Shields, B. J.; Liu, j.; Williams, M. J.; Zacuto, M. J.; Doyle, A. G. Mild, Redox-Neutral Formylation of Aryl Chlorides through the Photocatalytic Generation of Chlorine Radicals. Angew. Chem., Int. Ed. 2017, 56, 7191-7194. (i) Tellis, J. C.; Kelly, C. B.; Primer, D. N.; Jouffroy, M.; Patel, N. R.; Molander, G. A. Single-Electron Transmetalation via Photoredox/Nickel Dual Catalysis: Unlocking a New Paradigm for sp3-sp2 Cross-Coupling. Acc. Chem. Res. 2016, 49, 1429-1439. (j) Oderinde, M. S.; Frenette, M. A.; Aquila, B.; Robbins, D. W.; Johannes, J. W. Photoredox Mediated Nickel Catalyzed Cross-Coupling of Thiols With Aryl and Heteroaryl Iodides via Thiyl Radicals. J. Am. Chem. Soc. 2016, 138, 1760-1763. (k) Ahneman, D. T.; Doyle, A. G. C-H functionalization of amines with aryl halides by nickel-photoredox catalysis. Chem. Sci. 2016, 7, 7002-7006. (1) Shields, B. J.; Doyle, A. G. Direct C(sp3)-H Cross Coupling Enabled by Catalytic Generation of Chlorine Radicals. J. Am. Chem. Soc. 2016, 138, 12719-12722. (m) Gutierrez, O.; Tellis, J. C.; Primer, D. N.; Molander, G. A.; Kozlowski, M. C. Nickel-Catalyzed Cross-Coupling of Photoredox-Generated Radicals: Uncovering a General Manifold for Stereoconvergence in Nickel-Catalyzed Cross-Couplings. J. Am. Chem. Soc. 2015, 137, 4896-4899. (n) Xuan, J.; Zeng, T.-T.; Chen, J.-R.; Lu, L.-Q.; Xiao, W.-J. Room Temperature C-P Bond Formation Enabled by Merging Nickel Catalysis and Visible-Light-Induced Photoredox Catalysis. Chem. - Eur. J. 2015, 21, 4962-4965. (o) Tellis, J. C.; Primer, D. N.; Molander, G. A. Single-electron transmetalation in organoboron cross-coupling by photoredox/nickel dual catalysis. Science 2014, 345, 433-436. (p) Skubi, K. L.; Blum, T. R.; Yoon, T. P. Dual Catalysis Strategies in Photochemical Synthesis. Chem. Rev. 2016, 116, 10035-10074. (q) Ni, S.; Li, C.-X.; Mao, Y.; Han, J.; Wang, y.; Yan, H.; Pan, Y. Ni-catalyzed deaminative crosselectrophile coupling of Katritzky salts with halides via C-N bond activation. Sci. Adv. 2019, 5, No. eaaw9516. (r) Shen, Y.; Gu, Y.; Martin, R. sp3 C-H Arylation and Alkylation Enabled by the Synergy of Triplet Excited Ketones and Nickel Catalysts. J. Am. Chem. Soc. 2018, 140, 12200-12209. (s) García-Domínguez, A.; Mondal, R.; Nevado, C. DualPhotoredox/Nickel-CatalyzedThree-Component Carbofunctionalization of Alkenes. Angew. Chem., Int. Ed. 2019, 58, 12286-12290. (t) García-Domínguez, A.; Li, Z.; Nevado, C. Nickel-Catalyzed Reductive Dicarbofunctionalization of Alkenes. J. Am. Chem. Soc. 2017, 139, 6835-6838. (u) Li, Z.; García-Domínguez, A.; Nevado, C. Nickel-Catalyzed Stereoselective Dicarbofunctionalization of Alkynes. Angew. Chem., Int. Ed. 2016, 55, 6938-6941. (v) Luo, F. X.; Cao, Z.-C.; Zhao, H.-W.; Wang, D.; Zhang, Y.-F.; Xu, X.; Shi, Z.-J. Nickel-Catalyzed Oxidative Coupling of Unactivated C(sp3)-H Bonds in Aliphatic Amides with Terminal Alkynes. Organometallics 2017, 36, 18-21.

(5) (a) Huang, X.; Zhuang, T.; Kates, P. A.; Gao, H.; Chen, X.; Groves, J. T. Alkyl Isocyanates via Manganese-Catalyzed C–H Activation for the Preparation of Substituted Ureas. *J. Am. Chem. Soc.* **2017**, 139, 15407–15413. (b) Liu, W.; Cheng, M.-J.; Nielsen, R. J.; Goddard, W. A., III; Groves, J. T. Probing the C–O Bond-Formation Step in Metalloporphyrin-Catalyzed C–H Oxygenation Reactions. *ACS Catal.* **2017**, 7, 4182–4188. (c) Huang, X.; Groves, J. T. Taming Azide Radicals for Catalytic C–H Azidation. *ACS Catal.* **2016**, 6,

751-759. (d) Liu, W.; Groves, J. T. Manganese Catalyzed C-H Halogenation. Acc. Chem. Res. 2015, 48, 1727-1735.

(6) (a) Yamane, Y.; Yoshinaga, K.; Sumimoto, M.; Nishikata, T. Iron-Enhanced Reactivity of Radicals Enables C-H Tertiary Alkylations for Construction of Functionalized Quaternary Carbons. ACS Catal. 2019, 9, 1757-1762. (b) Pangia, T. M.; Davies, C. G.; Prendergast, J. R.; Gordon, J. B.; Siegler, M. A.; Jameson, G. N. L.; Goldberg, D. P. Observation of Radical Rebound in a Mononuclear Nonheme Iron Model Complex. J. Am. Chem. Soc. 2018, 140, 4191-4194. (c) Zaragoza, J. P. T.; Yosca, T. H.; Siegler, M. A.; Moënne-Loccoz, P.; Green, M. T.; Goldberg, D. P. Direct Observation of Oxygen Rebound with an Iron-Hydroxide Complex. J. Am. Chem. Soc. 2017, 139, 13640-13643. (d) Karimov, R. R.; Sharma, A.; Hartwig, J. F. Late Stage Azidation of Complex Molecules. ACS Cent. Sci. 2016, 2, 715-724. (e) Sharma, A.; Hartwig, J. F. Metal-catalysed azidation of tertiary C-H bonds suitable for late-stage functionalization. Nature 2015, 517, 600-604. (f) Krebs, C.; Galonić Fujimori, D.; Walsh, C. T.; Bollinger, J. M., Jr. Non-Heme Fe(IV)-Oxo Intermediates. Acc. Chem. Res. 2007, 40, 484-492.

(7) (a) Yoshino, T.; Matsunaga, S. Cobalt-Catalyzed C(sp3)-H Functionalization Reactions. Asian J. Org. Chem. 2018, 7, 1193-1205. (b) Lu, H.; Li, C.; Jiang, H.; Lizardi, C. L.; Zhang, X. P. Chemoselective Amination of Propargylic C(sp3)-H Bonds by Cobalt(II)-Based Metalloradical Catalysis. Angew. Chem., Int. Ed. 2014, 53, 7028-7032. (c) Belof, J. L.; Cioce, C. R.; Xu, X.; Zhang, X. P.; Space, B.; Woodcock, H. L. Characterization of Tunable Radical Metal-Carbenes: Key Intermediates in Catalytic Cyclopropanation. Organometallics 2011, 30, 2739-2746. (d) Lyaskovskyy, V.; Suarez, A. I. O.; Lu, H.; Jiang, H.; Zhang, X. P.; de Bruin, B. Mechanism of Cobalt(II) Porphyrin-Catalyzed C-H Amination with Organic Azides: Radical Nature and H-Atom Abstraction Ability of the Key Cobalt(III)-Nitrene Intermediates. J. Am. Chem. Soc. 2011, 133, 12264-12273. (e) Caselli, A.; Gallo, E.; Fantauzzi, S.; Morlacchi, S.; Ragaini, F.; Cenini, S. Allylic Amination and Aziridination of Olefins by Aryl Azides Catalyzed by CoII(tpp): A Synthetic and Mechanistic Study. Eur. J. Inorg. Chem. 2008, 2008, 3009-3019. (f) Harden, J. D.; Ruppel, J. V.; Gao, G.-Y.; Zhang, X. P. Cobalt-catalyzed intermolecular C-H amination with bromamine-T as nitrene source. Chem. Commun. 2007, 4644-4646. (g) Ragaini, F.; Penoni, A.; Gallo, E.; Tollari, S.; Li Gotti, C.; Lapadula, M.; Mangioni, E.; Cenini, S. Amination of Benzylic C-H Bonds by Arylazides Catalyzed by Co^{II}-Porphyrin Complexes: A Synthetic and Mechanistic Study. Chem. -Eur. J. 2003, 9, 249-259.

(8) (a) Tang, S.; Liu, Y.; Gao, X.; Wang, P.; Huang, P.; Lei, A. Multi-Metal-Catalyzed Oxidative Radical Alkynylation with Terminal Alkynes: A New Strategy for $C(sp^3)-C(sp)$ Bond Formation. J. Am. Chem. Soc. 2018, 140, 6006-6013. (b) Li, Z.-L.; Sun, K.-K.; Cai, C. Nickel-Catalyzed Cross-Dehydrogenative Coupling of α -C(sp³)– H Bonds in N-Methylamides with C(sp³)-H Bonds in Cyclic Alkanes. Org. Lett. 2018, 20, 6420-6424. (c) Tang, S.; Wang, P.; Li, H.; Lei, A. Multimetallic catalysed radical oxidative C(sp³)-H/ C(sp)-H cross-coupling between unactivated alkanes and terminal alkynes. Nat. Commun. 2016, 7, 11676. (d) Liu, D.; Li, Y.; Qi, X.; Liu, C.; Lan, Y.; Lei, A. Nickel-Catalyzed Selective Oxidative Radical Cross-Coupling: An Effective Strategy for Inert Csp3-H Functionalization. Org. Lett. 2015, 17, 998-1001. (e) Li, K.; Wu, Q.; Lan, J.; You, J. Coordinating activation strategy for $C(sp^3)-H/C(sp^3)-H$ cross-coupling to access β -aromatic α -amino acids. Nat. Commun. 2015, 6, 8404. (f) Zhou, L.; Tang, S.; Qi, X.; Lin, C.; Liu, K.; Liu, C.; Lan, Y.; Lei, A. Transition-Metal-Assisted Radical/Radical Cross-Coupling: A New Strategy to the Oxidative C(sp³)-H/N-H Cross-Coupling. Org. Lett. 2014, 16, 3404-3407. (g) Liu, D.; Liu, C.; Li, H.; Lei, A. Direct functionalization of tetrahydrofuran and 1,4-dioxane: nickel-catalyzed oxidative C(sp³)-H arylation. Angew. Chem., Int. Ed. 2013, 52, 4453-4456.

(9) (a) Zhang, Z.; Stateman, L. M.; Nagib, D. A. δ C–H (hetero)arylation via Cu-catalyzed radical relay. *Chem. Sci.* **2019**, *10*, 1207–1211. (b) Stateman, L. M.; Wappes, E. A.; Nakafuku, K. M.; Edwards, K. M.; Nagib, D. A. Catalytic β C–H amination via an

imidate radical relay. Chem. Sci. 2019, 10, 2693-2699. (c) Wang, F.; Chen, P.; Liu, G. Copper-Catalyzed Radical Relay for Asymmetric Radical Transformations. Acc. Chem. Res. 2018, 51, 2036-2046. (d) Stateman, L. M.; Nakafuku, K. M.; Nagib, D. A. Remote C-H Functionalization via Selective Hydrogen Atom Transfer. Synthesis 2018, 50, 1569-1586. (e) Kainz, Q. M.; Matier, C. D.; Bartoszewicz, A.; Zultanski, S. L.; Peters, J. C.; Fu, G. C. Asymmetric coppercatalyzed C-N cross-couplings induced by visible light. Science 2016, 351, 681-684. (f) Zhang, W.; Wang, F.; McCann, S. D.; Wang, D.; Chen, P.; Stahl, S. S.; Liu, G. Enantioselective cyanation of benzylic C-H bonds via copper-catalyzed radical relay. Science 2016, 353, 1014-1018. (g) Chikkade, P. K.; Kuninobu, Y.; Kanai, M. Coppercatalyzed intermolecular C(sp3)-H bond functionalization towards the synthesis of tertiary carbamates. Chem. Sci. 2015, 6, 3195-3200. (h) Tran, B. L.; Li, B.; Driess, M.; Hartwig, J. F. Copper-Catalyzed Intermolecular Amidation and Imidation of Unactivated Alkanes. J. Am. Chem. Soc. 2014, 136, 2555-2563. (i) Gephart, R. T., III; Warren, T. H. Copper-Catalyzed sp3 C-H Amination. Organometallics 2012, 31, 7728-7752. (j) Kharasch, M. S.; Sosnovsky, G. The Reactions of t-Butyl perbenzoate and Olefins-A stereospecific Reaction. J. Am. Chem. Soc. 1958, 80, 756-756.

(10) (a) Jenkins, C. L.; Kochi, J. K. Homolytic and ionic mechanisms in the ligand-transfer oxidation of alkyl radicals by copper(II) halides and pseudohalides. *J. Am. Chem. Soc.* 1972, 94, 856–865. (b) Kochi, J. K.; Jenkins, C. L. Ligand transfer of halides (chloride, bromide, iodide) and pseudohalides (thiocyanate, azide, cyanide) from copper(II) to alkyl radicals. *J. Org. Chem.* 1971, 36, 3095–3102. (c) Kochi, J. K.; Jenkins, C. L. Kinetics of ligand transfer oxidation of alkyl radicals. Evidence for carbonium ion intermediates. *J. Org. Chem.* 1971, 36, 3103–3111. (d) Kochi, J. K.; Subramanian, R. V. Studies of Ligand Transfer between Metal Halides and Free Radicals from Peroxides. *J. Am. Chem. Soc.* 1965, 87, 1508–1514.

(11) (a) Jang, E. S.; McMullin, C. L.; Käß, M.; Meyer, K.; Cundari, T. R.; Warren, T. H. Copper(II) Anilides in sp³ C-H Amination. J. Am. Chem. Soc. 2014, 136, 10930-10940. (b) Salvador, T. K.; Arnett, C. H.; Kundu, S.; Sapiezynski, N. G.; Bertke, J. A.; Boroujeni, M. R.; Warren, T. H. Copper Catalyzed sp³ C-H Etherification with Acyl Protected Phenols. J. Am. Chem. Soc. 2016, 138, 16580-16583. (c) Wiese, S.; Badiei, Y. M.; Gephart, R. T.; Mossin, S.; Varonka, M. S.; Melzer, M. M.; Meyer, K.; Cundari, T. R.; Warren, T. H. Catalytic C-H amination with unactivated amines through copper(II) amides. Angew. Chem., Int. Ed. 2010, 49, 8850-8855. (d) Aguila, M. J. B.; Badiei, Y. M.; Warren, T. H. Mechanistic Insights into C-H Amination via Dicopper Nitrenes. J. Am. Chem. Soc. 2013, 135, 9399-9406. (e) Gephart, R. T.; McMullin, C. L.; Sapiezynski, N. G.; Jang, E. S.; Aguila, M. J. B.; Cundari, T. R.; Warren, T. H. Reaction of CuI with Dialkyl Peroxides: CuII-Alkoxides, Alkoxy Radicals, and Catalytic C-H Etherification. J. Am. Chem. Soc. 2012, 134, 17350-17353. (f) Badiei, Y. M.; Dinescu, A.; Dai, X.; Palomino, R. M.; Heinemann, F. W.; Cundari, T. R.; Warren, T. H. Copper-nitrene complexes in catalytic C-H amination. Angew. Chem., Int. Ed. 2008, 47, 9961-9964. (g) Gephart, R. T.; Huang, D. L.; Aguila, M. J. B.; Schmidt, G.; Shahu, A.; Warren, T. H. Catalytic C-H Amination with Aromatic Amines. Angew. Chem., Int. Ed. 2012, 51, 6488-6492.

(12) (a) Okoromoba, O. E.; Jang, E. S.; McMullin, C.; Cundari, T.; Warren, T. H.Copper Catalyzed sp³ C-H α-Acetylation. 2019, chemrxiv.11407116.v1. *ChemRxiv Preprint*. https://doi.org/10.26434/chemrxiv.11407116.v1. (b) Vasilopoulos, A.; Zultanski, S. L.; Stahl, S. S. Feedstocks to Pharmacophores: Cu-Catalyzed Oxidative Arylation of Inexpensive Alkylarenes Enabling Direct Access to Diarylalkanes. *J. Am. Chem. Soc.* 2017, 139, 7705–7708. (c) Zhang, W.; Chen, P.; Liu, G. Copper-Catalyzed Arylation of Benzylic C–H bonds with Alkylarenes as the Limiting Reagents. *J. Am. Chem. Soc.* 2017, 139, 7709–7712.

(13) A preprint of this manuscript has appeared on ChemRxiv: Bakhoda, A.; Wiese, S.; Greene, C.; Figula, B. C.; Bertke, J. A.; Warren, T. H. Radical Capture at Ni(II) Complexes: C-C, C-N, and C-O Bond Formation. 2019, chemrxiv.8115860.v1. *ChemRxiv Preprint*. https://doi.org/10.26434/chemrxiv.8115860.v1

(14) (a) Wiese, S.; McAfee, J. L.; Pahls, D. R.; McMullin, C. L.; Cundari, T. R.; Warren, T. H. C–H Functionalization Reactivity of a Nickel–Imide. *J. Am. Chem. Soc.* **2012**, *134*, 10114–10121. (b) Wiese, S.; Aguila, M. J. B.; Kogut, E.; Warren, T. H. β -Diketiminato Nickel Imides in Catalytic Nitrene Transfer to Isocyanides. *Organometallics* **2013**, *32*, 2300–2308.

(15) Melzer, M. M.; Jarchow-Choy, S.; Kogut, E.; Warren, T. H. Reductive Cleavage of O-, S-, and N-Organonitroso Compounds by Nickel(I) β -Diketiminates. *Inorg. Chem.* **2008**, 47, 10187–10189.

(16) (a) Schubert, E. M. Utilizing the Evans method with a superconducting NMR spectrometer in the undergraduate laboratory. *J. Chem. Educ.* **1992**, *69*, *62*. (b) Evans, D. F. The determination of the paramagnetic susceptibility of substances in solution by nuclear magnetic resonance. *J. Chem. Soc.* **1959**, 2003.

(17) (a) Zhang, X.; Emge, T. J.; Ghosh, R.; Krogh-Jespersen, K.; Goldman, A. S. Reaction of Nitromethane with an Iridium Pincer Complex. Multiple Binding Modes of the Nitromethanate Anion. Organometallics 2006, 25, 1303–1309. (b) Ito, H.; Ito, T. Syntheses, Characterization, and Molecular Structures of Nitroalkanato Nickel-(II), Zinc(II), and Cadmium(II) Complexes with Tetraazacycloalkanes. Chem. Lett. 1985, 14, 1251–1254.

(18) (a) Zabicky, J., Ed. The Chemistry of Metal Enolates; John Wiley and Sons, Ltd.: West Sussex, 2009. (b) Knochel, P., Ed. Comprehensive Organic Synthesis II; Elsevier Ltd.: Amsterdam, 2014. (c) Bailey, W. D.; Gagnon, N. L.; Elwell, C. L.; Cramblitt, A. C.; Bouchey, C. J.; Tolman, W. B. Revisiting the Synthesis and Nucleophilic Reactivity of an Anionic Copper Superoxide Complex. Inorg. Chem. 2019, 58, 4706-4711. (d) Cámpora, J.; Maya, C. M.; Palma, P.; Carmona, E.; Gutiérrez-Puebla, E.; Ruiz, C. Synthesis and Aldol Reactivity of Oand C-Enolate Complexes of Nickel. J. Am. Chem. Soc. 2003, 125, 1482-1483. (e) Burkhardt, E. R.; Bergman, R. G.; Heathcock, C. H. Synthesis and reactions of nickel and palladium carbon-bound enolate complexes. Organometallics 1990, 9, 30-44. (f) Belderraín, T. R.; Knight, D. A.; Irvine, D. j.; Paneque, M.; Poveda, M. l.; Carmona, E. Ethoxycarbonyl-, cyano- and methoxy-methyl complexes of nickel(II) and their carbonylation reactions. J. Chem. Soc., Dalton Trans. 1992, 1491-1495. (g) Bonamico, M.; Dessy, G.; Fares, V.; Scaramuzza, L. Structural studies of metal complexes with ω -nitroacetophenone. Crystal structures of bis-(\omega-nitroacetophenonato)copper(II), and of its addition complexes with 2- and 4-methylpyridine (α -and γ picoline). J. Chem. Soc., Dalton Trans. 1972, 2477-2483.

(19) (a) Haidasz, E. A.; Meng, D. A.; Amorati, R.; Baschieri, A.; Ingold, K. U.; Valgimigli, L.; Pratt, D. A. Acid Is Key to the Radical-Trapping Antioxidant Activity of Nitroxides. *J. Am. Chem. Soc.* 2016, 138, 5290–5298. (b) Ross, S. D.; Finkelstein, M.; Petersen, R. C. The Electrochemical Degradation of Quaternary Ammonium Salts. II. The Mechanism of the Coupling Reaction. *J. Am. Chem. Soc.* 1960, 82, 1582–1585.

(20) (a) Khake, S. M.; Chatani, N. Chelation-Assisted Nickel-Catalyzed C—H Functionalizations. *Trends Chem.* **2019**, *1*, 524–539. (b) Liu, C.; Liu, D.; Lei, A. Recent Advances of Transition-Metal Catalyzed Radical Oxidative Cross-Couplings. *Acc. Chem. Res.* **2014**, 47, 3459–3470. (c) Gossage, R. A.; Van De Kuil, L. A.; Van Koten, G. Diaminoarylnickel(II) "Pincer" Complexes: Mechanistic Considerations in the Kharasch Addition Reaction, Controlled Polymerization, and Dendrimeric Transition Metal Catalysts. *Acc. Chem. Res.* **1998**, 31, 423–431.

(21) (a) Liu, S.; Qi, X.; Bai, R.; Lan, Y. Theoretical Study of Ni-Catalyzed C-N Radical-Radical Cross-Coupling. *J. Org. Chem.* **2019**, 84, 3321–3327. (b) Omer, H. M.; Liu, P. Computational Study of Ni-Catalyzed C-H Functionalization: Factors That Control the Competition of Oxidative Addition and Radical Pathways. *J. Am. Chem. Soc.* **2017**, 139, 9909–9920.

(22) Engel, P. S. Mechanism of the thermal and photochemical decomposition of azoalkanes. *Chem. Rev.* **1980**, *80*, 99–150.